# Finite Element Model Updating of a Space Frame Bridge with Mobile Sensing Data

Dapeng Zhu [a], Chia-Hung Fang [a], Chunhee Cho [a], Jiajie Guo [b], Yang Wang *[a], Kok-Meng Lee [b]
[a] School of Civil and Environmental Eng., Georgia Inst. of Tech., Atlanta, GA 30332, USA
[b] George W. Woodruff School of Mechanical Eng., Georgia Inst. of Tech., Atlanta, GA 30332, USA

## ABSTRACT

This research investigates the field performance of a mobile sensor network designed for structural health monitoring. Each mobile sensing node (MSN) is a small magnet-wheeled tetherless robot that carries sensors and autonomously navigates on a steel structure. A four-node mobile sensor network is deployed for navigating on the top plane of a space frame bridge. With little human effort, the MSNs navigate to different sections of the steel bridge, attach accelerometers, and measure structural vibrations at high spatial resolution. Using high-resolution data collected by a small number of MSNs, detailed modal characteristics of the bridge are identified. A finite element model for the bridge is constructed according to structural drawings, and updated using modal characteristics extracted from mobile sensing data.

**Keywords:** mobile sensor network, mobile sensing node (MSN), system identification, modal analysis, finite element model updating.

## 1. INTRODUCTION

As civil structures can be continuously exposed to harsh outdoor environment, structural safety condition may deteriorate significantly throughout the service life. Taking bridges as an example, the ASCE 2009 report card concluded that more than one fourth of the bridges in the United States are categorized as structurally deficient or functionally obsolete [1]. In order to improve the safety assessment of civil structures, structural health monitoring (SHM) systems have been widely explored for monitoring structural performance and identifying potential damage [2, 3]. Traditionally, coaxial cables are used to transmit sensor data. However, the high cost and time consumption associated with cable installation hinders widespread adoption of SHM systems [4, 5]. In order to overcome the difficulties, many academic and commercial wireless sensor prototypes for structural monitoring have been developed and validated in laboratory and field testing [6]. Nevertheless, for accurate structural system identification, dense deployment of high-precision accelerometers is usually required. Such an accelerometer typically costs at least a few hundred dollars each. Therefore, the cost for SHM systems is still high, even using wireless data acquisition. To overcome this difficulty, mobile sensor networks can be pursued [7]. A mobile sensor network contains multiple mobile sensing nodes (MSNs). Each MSN is a miniature robot equipped with smart wireless sensors. The MSN explores its surroundings and exchanges information with peers through wireless communication. Compared with static wireless sensor deployment, mobile sensor networks offer flexible deployment and high spatial resolution for structural system identification, while consuming little human effort.

Over the past few decades, many efforts have been made in developing miniature agile robots for engineering applications. For example, to inspect the inner casing of ferromagnetic pipes with complex-shaped structures, a compact robot with two magnetic wheels in a motorbike arrangement has been developed [8]. Wall climbing robots have been developed for navigating on flat surfaces in any orientation, utilizing elastomeric dry adhesion [9] or claw gripping [10]. Some researchers have incorporated mobility with traditional sensors for structural monitoring. For example, a beam-crawler has been developed for wirelessly powering and interrogating battery-less peak-strain sensors; the crawler is

* yang.wang@ce.gatech.edu; phone 1 404 894-1851; fax 1 404 894-2278; http://www.ce.gatech.edu/~ywang

capable of moving along the flange of an I-beam by wheels [11]. More recently, a remotely-controlled model helicopter has been demonstrated for charging and communicating with wireless sensors as a mobile host [12]. However, to the best of our knowledge, mobile sensor networks with dynamic reconfiguration have rarely been explored by researchers for structural monitoring.

This research investigates the field performance of a mobile sensor network designed for structural monitoring. Each MSN, developed by researchers at Georgia Tech [13-15], is a small magnet-wheeled tetherless robot that carries sensors and autonomously navigates on a steel structure. In the field testing, a four-node mobile sensor network is deployed for navigating on the top plane of a space frame bridge. The MSNs navigate to different sections of the steel bridge, attach accelerometers, and measure structural vibrations at high spatial resolution. Detailed modal characteristics of the bridge are extracted from the mobile sensing data. A finite element model for the bridge is constructed according to structural drawings, and updated by the modal parameters. The rest of the paper is organized as follows. Section 2 describes the testbed space frame bridge and experimental setup. Section 3 shows example measurement data and modal analysis results. Section 4 presents the FE model updating process and the updated structural parameters. Finally, a summary and discussion are provided.

## 2. FIELD TESTING OF MOBILE SENSING NODES

The testbed bridge is located on Georgia Tech campus, connecting the Manufacturing Research Center (MARC) with the Manufacturing Related Disciplines Complex (MRDC) (Fig. 1). This bridge is a simply supported space frame structure, with hinge connections on the MRDC side and roller connections on the MARC side. The bridge consists of eleven chord units. Diagonal tension bars are deployed in two vertical side planes and the top horizontal plane, and each floor unit contains a diagonal bracing tube. Detailed dimensions of the bridge are listed in Table 1.

The MSN used in this study is a miniature magnet-wheeled climbing robot capable of navigating on steel structures, as well as attaching/detaching an accelerometer onto/from structural surface for accurate vibration measurement. Design and implementation of the MSN can be found in [13-15]. The accelerometer (Silicon Designs 2260-010) equipped on each MSN has a frequency bandwidth of 0-300 Hz and a measurement range of ±2g. Each MSN includes a signal conditioning module for filtering and amplifying the accelerometer signal. The cutoff frequency and amplification gain are set to 25Hz and ×20, respectively. Sampling rate is set to 200Hz.

In the field testing, four MSNs are adopted to navigate on the top plane of the bridge and measure structural vertical vibrations. As shown in Fig. 2(a), a total of five measurement configurations are allocated on the top plane of the bridge frame. Each configuration consists of four measurement locations, one for every MSN. Locations at south side of the frame are marked with letter ‘S’, and locations at north side are marked with letter ‘N’. Wirelessly controlled by a laptop server located on the floor level at one side of the bridge (Fig. 2(b)), the MSNs start from the inclined members


Fig. 1. Photo of the space frame bridge on Georgia Tech campus.

Table 1. Dimensions of the steel bridge

| *Dimension* | | *Value* |
|---|---|---|
| Length | | $11 \times 2.74$m = 30.2m (99 ft) |
| Width | | 2.13m (7 ft) |
| Height | | 2.74m (9 ft) |
| Concrete floor slab thickness | | 0.139 m (5.5 in) |
| Cross section and thickness of square tubes | Top-plane longitudinal | 0.152 m $\times$ 0.152 m $\times$ 0.0080 m (6 in $\times$ 6 in $\times$ 5/16 in) |
| | Bottom-plane longitudinal | 0.152 m $\times$ 0.152 m $\times$ 0.0095 m (6 in $\times$ 6 in $\times$ 3/8 in) |
| | Others | 0.152 m $\times$ 0.152 m $\times$ 0.0064 m (6 in $\times$ 6 in $\times$ 1/4 in) |

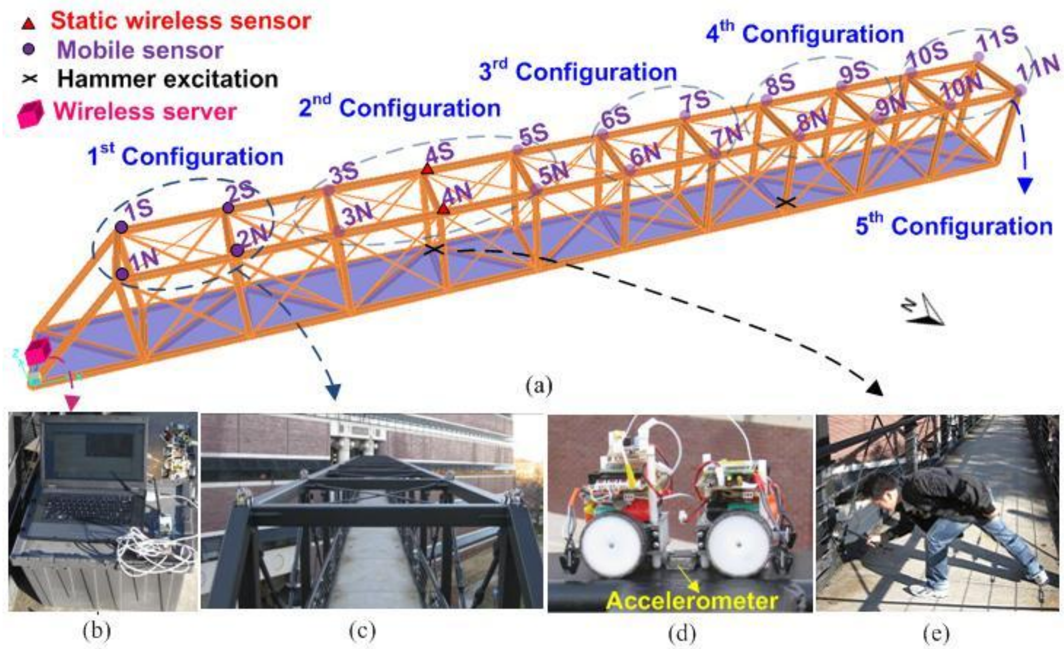


Fig. 2. Experimental setup for mobile sensor testing: (a) 3D illustration of five measurement configurations for the MSNs; (b) a laptop as the wireless server; (c) four MSNs deployed at the 1st configuration; (d) an MSN attaches an accelerometer onto the structural surface; (e) a hammer impact is being applied.

on MRDC side, move to the 1st configuration, and attach accelerometers onto the structural surface (Fig. 2(c)). Structural vibration data are recorded by the MSNs, and wirelessly transmitted to the server. Fig. 2(d) shows an MSN taking measurement with the accelerometer attached on structural surface. After finishing measurement at one configuration, the four MSNs move to the next configuration, until they finish all configurations. Measurement configurations for the MSNs do not contain locations 4S and 4N, where static wireless sensing nodes are mounted as reference nodes for assembling mode shapes of the entire bridge. For vibration measurement at each configuration, hammer impact is first applied at the floor below 4S for exciting the bridge and collecting acceleration data, and then another impact is applied below 8N. Fig. 2(e) shows the photo of a hammer impact being applied at the location below 4S. The impact hammer is a 3-lb hammer manufactured by PCB Piezotronics.

For comparison, another set of instrumentation is performed entirely with static wireless sensors. The sensors are installed at measurement locations on the top plane of the bridge frame (Fig. 3). Narada wireless sensing units, developed by researchers at the University of Michigan, are deployed in the static sensor instrumentation. Performance

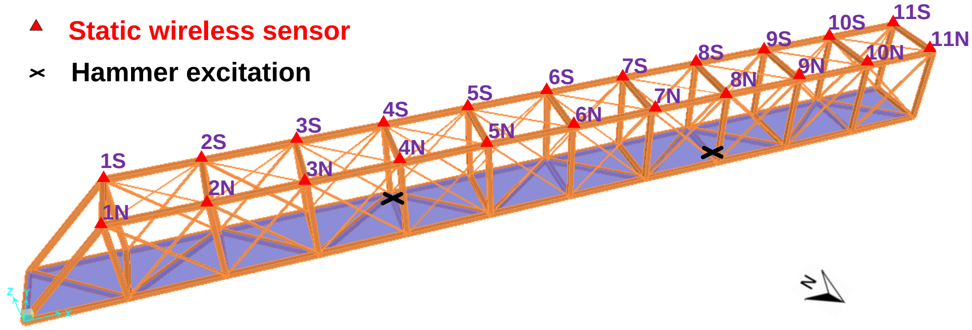


Fig. 3. Experimental setup for the testing with static wireless sensors.

of the Narada system has been validated in a number of previous studies [16-18]. Silicon Designs 2260-010 accelerometers are also used in static sensor instrumentation, for measuring vertical bridge vibrations. Other experimental setups remain the same as in mobile sensor test. The static sensor data can serve as a baseline for evaluating quality of the mobile sensing data.

## 3. EXAMPLE MOBILE SENSOR DATA AND MODAL ANALYSIS RESULTS

Fig. 4 presents example acceleration data recorded by MSNs at locations 7N and 9N, as well as the corresponding frequency spectra when the hammer impact is applied on the floor below location 8N. Fig. 5 presents the acceleration data and frequency spectra recorded by static wireless sensors at the same measurement and hammer impact locations. Similar wave forms are observed between the time history plots in Fig. 4 and Fig. 5, for both pairs of measurement locations. Furthermore, similar peaks are observed between frequency spectra of the mobile sensor data and static wireless sensor data. The comparison confirms the reliable quality of the mobile sensor data.

The eigensystem realization algorithm (ERA) [19] is applied to the impulse response functions obtained from mobile

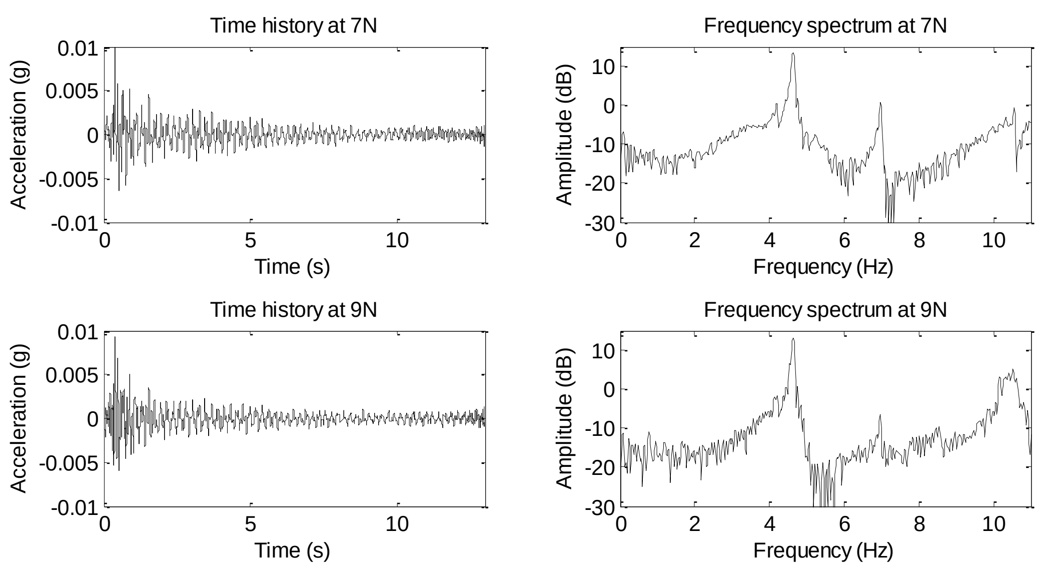


Fig. 4. Example vibration records and corresponding frequency spectra recorded by mobile sensors when hammer impact is applied on the floor below location 8N.

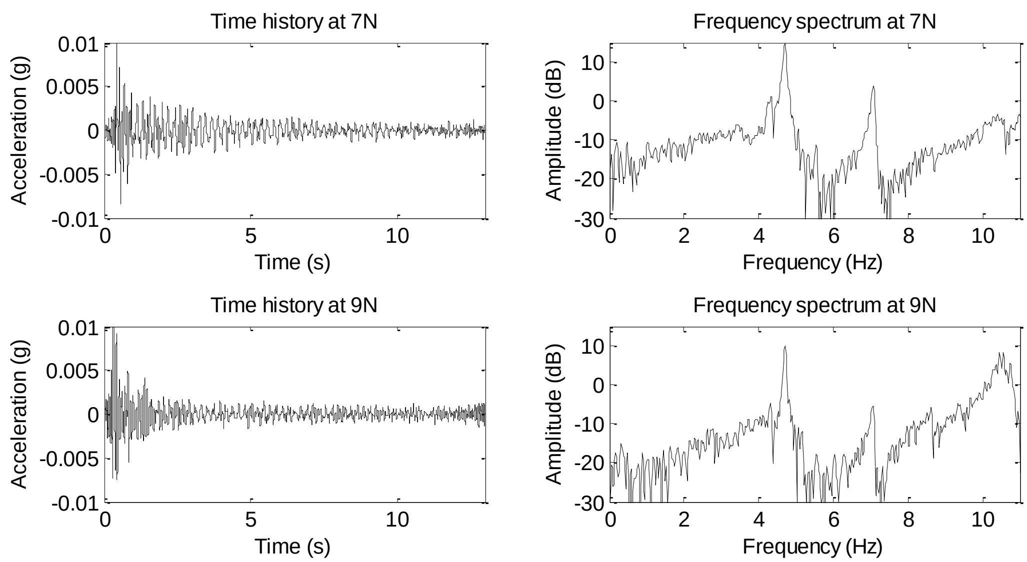


Fig. 5. Example vibration records and corresponding frequency spectra recorded by static sensors when hammer impact is applied on the floor below location 8N.

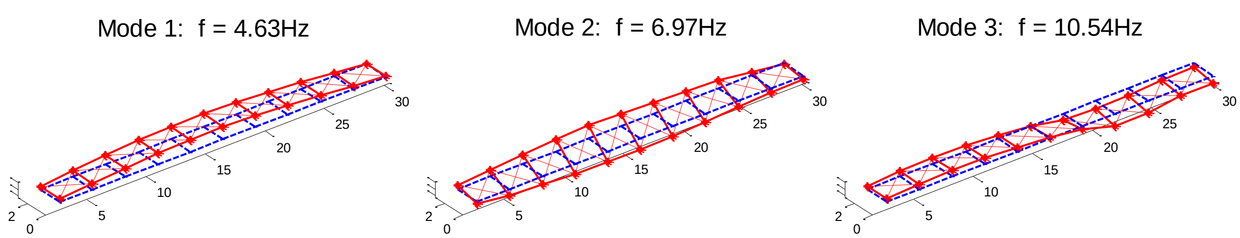


Fig. 6. First three mode shapes of the bridge extracted from mobile sensing data with hammer impact excitation.

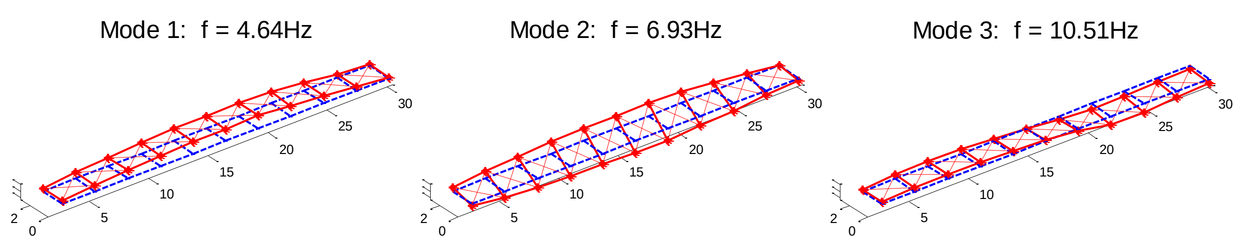


Fig. 7. First three mode shapes of the bridge extracted from static sensor data with hammer impact excitation.

sensing data, for extracting modal characteristics at each configuration. In order to eliminate noise effect, structural vibration data with hammer impact under 4S are used to extract modal characteristics of configurations 1~2, while data with hammer impact under 8N are used for configurations 3~5. Mode shapes of the entire bridge are then assembled through the reference nodes with two static wireless sensors (Fig. 2(a)). Fig. 6 shows the first three assembled mode shapes. Because the MSNs measure vertical bridge accelerations, only vertical components of each mode shape can be extracted. Similarly, the ERA is also applied to the impulse response functions obtained from static wireless sensor data. Modal characteristics are extracted and shown in Fig. 7. Comparison between Fig. 6 and Fig. 7 shows that the natural frequencies and mode shapes extracted from mobile sensing data and static wireless sensor data are very close. Therefore, it can be concluded that the four-node mobile sensor network provides adequately high-precision measurement and spatial resolution with very little human effort.

## 4. FINITE ELEMENT MODEL UPDATING

A finite element (FE) model of the bridge is built in OpenSees according to structural drawings (Fig. 8(a)). All steel frame members are modeled as elastic beam-column elements, and diagonal tension bars on the side and top planes are modeled as 3D truss elements. The concrete slab in this structure is connected with bottom-plane frame members by shear studs, through which bending moment can be transferred. To consider stiffness provided by the concrete slab, shell elements are adopted for modeling the concrete slab. For boundary conditions, ideal hinges or rollers are usually used in structural design and analysis, but such ideal conditions do not exist in reality and may affect dynamic behavior of the FE model. To describe realistic support conditions, the hinge support at MRDC side is replaced by a rigid link in longitudinal direction, and springs in transverse and vertical directions (Fig. 8(b)). Meanwhile, the roller support at MARC side is replaced by springs in transverse and vertical directions (Fig. 8(c)).

Important structural parameters, including material properties and boundary stiffnesses, are selected for FE model updating (Table 2). Each of the material property parameters (e.g. concrete stiffness) applies to structural components spread out on the entire bridge. No spatial variation of these parameters at different portions of the bridge is considered in this preliminary work. As a result, changes in these parameters mostly lead to changes in natural frequencies, instead of changes in mode shapes that mainly reflect relative ratios among different portions of the structure. If mode shape sensitivity to the parameters is to be pursued in future work, spatial variation of mass and stiffness parameters should be considered in model updating. Due to the insensitivity of bridge mode shapes against the updating parameters listed in Table 2, only natural frequencies are considered in the optimization objective. The formulation minimizes the difference between three experimental natural frequencies extracted from mobile sensing data and corresponding frequencies provided by FE model:

$$\text{minimize} \quad \sum_{i=1}^{3}\left(\frac{f_{FE,i}-f_{M,i}}{f_{M,i}}\right)^2 \tag{1}$$

where $f_{FE,i}$ denotes the $i$-th natural frequency provided by the FE model, and $f_{M,i}$ denotes the frequency extracted from mobile sensing data. Using MATLAB optimization toolbox [20], an interior-point optimization procedure is performed.

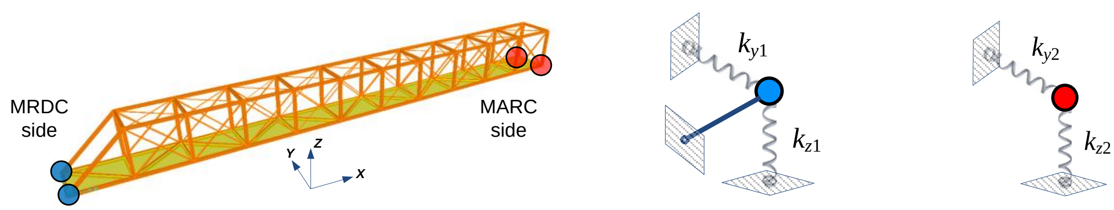


(a) (b) (c)

Fig. 8. FE model for the steel bridge: (a) 3D view of the bridge model; (b) support condition at MRDC side for model updating; (c) support condition at MARC side for model updating.

Table 2. Selected parameters for model updating

| *Updating parameters* | | | *Initial value* | *Optimal value* |
|---|---|---|---|---|
| Concrete slab | Density (kg/m$^3$) | | $2.48\times10^3$ | $2.64\times10^3$ |
| | Elastic modulus (N/m$^2$) | | $2.07\times10^{10}$ | $1.65\times10^{10}$ |
| Steel | Density (kg/m$^3$) | | $7.87\times10^3$ | $8.26\times10^3$ |
| | Elastic modulus ( N/m$^2$) | Frame tubes | $2.0\times10^{11}$ | $1.9\times10^{11}$ |
| | | Tension bars | $2.0\times10^{11}$ | $2.0\times10^{11}$ |
| Support | Transverse $k_{y1}$ (kN/m) | | $3.50\times10^4$ | $2.45\times10^4$ |
| | Vertical $k_{z1}$ (kN/m) | | $8.76\times10^4$ | $1.40\times10^5$ |
| | Transverse $k_{y2}$ (kN/m) | | $3.50\times10^4$ | $2.45\times10^4$ |
| | Vertical $k_{z2}$ (kN/m) | | $8.76\times10^4$ | $1.40\times10^5$ |

The final updated structural parameters are listed in the last column of Table 2.

The first five natural frequencies and mode shapes of the updated FE model are shown in Fig. 9. For each mode, the left plot shows the mode shape of the entire bridge model in 3D view. The right plot shows only the vertical components of the mode shape at the top plane, for comparison with the experimental mode shape from mobile sensing data. The Z/Y ratio equals the maximum vertical magnitude in the mode shape vector divided by the maximum lateral magnitude. Mode shapes with small Z/Y ratios have trivial vertical direction components, including Lateral-1 and Lateral-2 modes. These two mode shapes are not reliably captured by the MSNs, because only vertical structural vibrations are measured. Mode shapes with relatively large Z/Y ratios are easily captured by MSNs. By comparing Fig. 6 and Fig. 9, it can be observed that the Vertical-1 shape from the FE model corresponds to Mode-1 extracted from experimental data, Torsional-1 corresponds to Mode-2, and Vertical-2 corresponds to Mode-3.

Table 3 shows modal characteristics extracted from the mobile sensing data, as compared with these from FE model. The largest frequency difference is 8.66% for the initial FE model, and reduces to 4.15% for the updated FE model. The modal assurance criterion (MAC) values are calculated to compare the experimental mode shapes with these of both initial and updated FE models. The values are close to 1 for Mode-1 and Mode-2, and about 0.8 for Mode-3. Besides, the MAC values are almost the same for the initial and updated FE models, which confirms that mode shapes are not sensitive to the updating parameters. In summary, both the natural frequencies and mode shapes of the updated FE model are fairly close to experimental results from mobile sensor data.

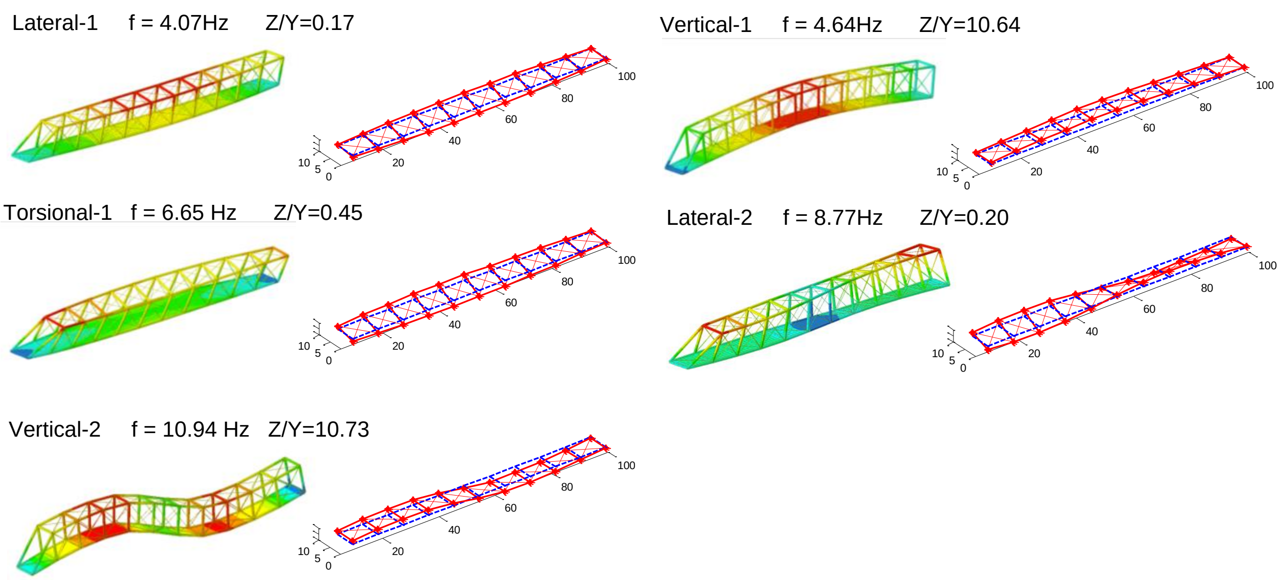


Fig. 9. First five mode shapes of the FE model.

Table 3. Comparison of modal characteristics extracted from mobile sensing data and FE model

| *Mode No.* | *Experiment* | *Initial FE Model* | | | *Updated FE Model* | | |
|---|---|---|---|---|---|---|---|
| | *Freq. (Hz)* | *Freq. (Hz)* | *Difference* | *MAC value* | *Freq. (Hz)* | *Difference* | *MAC value* |
| 1 | 4.63 | 4.85 | 4.53% | 0.99 | 4.64 | 0.02% | 0.99 |
| 2 | 6.97 | 6.78 | 2.17% | 0.96 | 6.65 | 4.15% | 0.97 |
| 3 | 10.53 | 11.42 | 8.66% | 0.79 | 10.94 | 4.07% | 0.78 |

## 5. CONCLUSION AND FUTURE WORK

This research illustrates the field application of a mobile sensor network on a simply supported space frame bridge. A four-node mobile sensor network is employed to navigate on the top plane of the bridge and measure structural vibrations with high spatial resolution. Using data collected by four MSNs, detailed modal characteristics of the bridge are identified and validated with reference static sensors. An FE model for the bridge is built according to the structural drawings and updated based on the modal characteristics extracted from the mobile sensing data. The updated FE model provides modal characteristics that are close to these extracted from mobile sensing data. Future development will be conducted to improve the mobile sensing nodes for navigating on more complicated real-world structures. In addition, substructure-based FE model updating algorithms will be explored to best utilize the mobile sensing data.


## ACKNOWLEDGEMENT

This research is partially sponsored by the National Science Foundation, under grant number CMMI-0928095 (Sensors and Sensing Systems). The authors gratefully acknowledge the support.


## REFERENCES


[1] ASCE, *Report Card for America's Infrastructure*, American Society of Civil Engineers, Reston, VA (2009).

[2] Ko, J.M. and Ni, Y.Q., "Technology developments in structural health monitoring of large-scale bridges," *Eng. Struct.*, 27(12), 1715-1725 (2005).

[3] Farrar, C.R., Sohn, H., Hemez, F.M., Anderson, M.C., Bement, M.T., Cornwell, P.J., Doebling, S.W., Schultze, J.F., Lieven, N. and Robertson, A.N., *Damage Prognosis: Current Status and Future Needs*. Report No. LA-14051-MS, Los Alamos National Laboratory, Los Alamos, NM (2003).

[4] Çelebi, M., *Seismic Instrumentation of Buildings (with Emphasis on Federal Buildings)*. Report No. 0-7460-68170, United States Geological Survey, Menlo Park, CA (2002).

[5] Straser, E.G. and Kiremidjian, A.S., *A Modular, Wireless Damage Monitoring System for Structures*. Report No. 128, John A. Blume Earthquake Eng. Ctr., Stanford University, Stanford, CA (1998).

[6] Lynch, J.P. and Loh, K.J., "A summary review of wireless sensors and sensor networks for structural health monitoring," *Shock Vib. Dig.*, 38(2), 91-128 (2006).

[7] Akyildiz, I.F., Su, W., Sankarasubramaniam, Y. and Cayirci, E., "A survey on sensor networks," *IEEE Commun. Mag.*, 40(8), 102-114 (2002).

[8] Tache, F., Fischer, W., Caprari, G., Siegwart, R., Moser, R. and Mondada, F., "Magnebike: A magnetic wheeled robot with high mobility for inspecting complex-shaped structures," *J. Field Robot.*, 26(5), 453-476 (2009).

[9] Murphy, M.P. and Sitti, M., "Waalbot: an agile small-scale wall-climbing robot utilizing dry elastomer adhesives," *IEEE-ASME T. Mech.*, 12(3), 330-338 (2007).

[10] Provancher, W.R., Jensen-Segal, S.I. and Fehlberg, M.A., "ROCR: An Energy-Efficient Dynamic Wall-Climbing Robot," *IEEE-ASME T. Mech.*, 16(5), 897-906 (2011).

[11] Huston, D.R., Esser, B., Gaida, G., Arms, S.W. and Townsend, C.P., "Wireless inspection of structures aided by robots," *Proceedings of SPIE, Health Monitoring and Management of Civil Infrastructure Systems*, Newport Beach, CA, March 6, 2001.

[12] Todd, M., Mascarenas, D., Flynn, E., Rosing, T., Lee, B., Musiani, D., Dasgupta, S., Kpotufe, S., Hsu, D., Gupta, R., Park, G., Overly, T., Nothnagel, M. and Farrar, C., "A different approach to sensor networking for SHM: remote powering and interrogation with unmanned aerial vehicles," *Proceedings of the 6th International Workshop on Structural Health Monitoring*, Stanford, CA, September 11 - 13, 2007.

[13] Lee, K.-M., Wang, Y., Zhu, D., Guo, J. and Yi, X., "Flexure-based mechatronic mobile sensors for structure damage detection," *Proceedings of the 7th International Workshop on Structural Health Monitoring*, Stanford, CA, USA, September 9 - 11, 2009.

[14] Guo, J., Lee, K.-M., Zhu, D., Yi, X. and Wang, Y., "Large-deformation analysis and experimental validation of a flexure-based mobile sensor node," *IEEE-ASME T. Mech.*, in print, dx.doi.org/10.1109/TMECH.2011.2107579.

[15] Zhu, D., Yi, X., Wang, Y., Lee, K.-M. and Guo, J., "A mobile sensing system for structural health monitoring: design and validation," *Smart Mater. Struct.*, 19(5), 055011 (2010).
[16] Zimmerman, A.T., Shiraishi, M., Swartz, R.A. and Lynch, J.P., "Automated modal parameter estimation by parallel processing within wireless monitoring systems," *J. Infrastruct. Syst.*, 14(1), 102-113 (2008).
[17] Swartz, R.A., Jung, D., Lynch, J.P., Wang, Y., Shi, D. and Flynn, M.P., "Design of a wireless sensor for scalable distributed in-network computation in a structural health monitoring system," *Proceedings of the 5th International Workshop on Structural Health Monitoring*, Stanford, CA, September 12 - 14, 2005.
[18] Swartz, R.A. and Lynch, J.P., "Strategic network utilization in a wireless structural control system for seismically excited structures," *J. Struct. Engrg.*, 135(5), 597-608 (2009).
[19] Juang, J.N. and Pappa, R.S., "An eigensystem realization algorithm for modal parameter identification and modal reduction," *J. Guid. Control Dynam.* , 8(5), 620-627 (1985).
[20] MathWorks Inc., *Optimization Toolbox™ User's Guide*, MathWorks Inc., Natick, MA (2011).